IJMMM International Journal of Minerals, Metallurgy and Materials 矿物冶金与材料学报（英文版）

Influencing factors and mechanism of iodine-induced stress corrosion cracking of zirconium alloy cladding: A review

Yusha Li, Changchun Ge, Yanhong Liu, Guangbin Li, Xiaoxu Dong, Zongxing Gu, and Yingchun Zhang

Cite this article as:
Yusha Li, Changchun Ge, Yanhong Liu, Guangbin Li, Xiaoxu Dong, Zongxing Gu, and Yingchun Zhang, Influencing factors and mechanism of iodine-induced stress corrosion cracking of zirconium alloy cladding: A review, *Int. J. Miner. Metall. Mater.*, 29(2022), No. 4, pp. 586-598. https://doi.org/10.1007/s12613-022-2431-6

View the article online at SpringerLink or IJMMM Webpage.

International Journal of Minerals, Metallurgy and Materials
Volume 29, Number 4, April 2022, Page 586
https://doi.org/10.1007/s12613-022-2431-6

Invited Review

Influencing factors and mechanism of iodine-induced stress corrosion cracking of zirconium alloy cladding: A review

Yusha Li[1)], *Changchun Ge*[1),✉], *Yanhong Liu*[2)], *Guangbin Li*[1)], *Xiaoxu Dong*[1)], *Zongxing Gu*[1)], *and Yingchun Zhang*[1),✉]

1) School of Materials Science and Engineering, University of Science and Technology Beijing, Beijing 100083, China
2) State Power Investment Corporation Science and Technology Research Institute, Beijing 100029, China
(Received: 29 September 2021; revised: 28 January 2022; accepted: 29 January 2022)

Abstract: Failure of the zirconium alloy claddings due to iodine-induced stress corrosion cracking (I-SCC) will increase the risk of fission product leakage. The progress of I-SCC has been comprehensively investigated in a massive amount of published literature. For a comprehensive understanding of I-SCC, this review focuses on summarizing the mechanisms and influencing factors of I-SCC. Results show that micropits are formed on the surface of zirconium alloys due to the reaction between iodine and zirconium, and then small pits gradually gather to form pit clusters. Cracks are easily generated in pit clusters and propagate along the grain boundary. After reaching a particular condition, the crack will transform into transgranular direction propagation. As the crack develops, it finally becomes a ductile fracture. We also summarize various factors that may affect I-SCC. The specific cracking conditions are linked to elements, such as iodine concentration, temperature, microstructure, and alloying elements. Nonetheless, the improvement of the I-SCC resistance of zirconium alloys needs to be further explored. More attention can be paid to material properties, such as alloying elements, microstructure, and surface treatment, to improve the I-SCC resistance of zirconium alloys.

Keywords: iodine-induced stress corrosion cracking; zirconium; fracture

1. Introduction

Nuclear power generation was used as the primary commercial power production in the 1950s because nuclear power is efficient and reliable [1–2]. Accordingly, several studies have been conducted. Nuclear power is economically feasible and meets more than 20% of the world's demand for electricity [3]. Additionally, nuclear power helps reduce environmental degradation caused by power generation activities [4]. As such, nuclear safety is always considered and emphasized. The Chernobyl incident and Fukushima Daiichi accident remind the world that strengthening nuclear safety consciousness is not an option but a necessity [5–7]. The fission of U atoms produces radioactive materials, such as neutrons, γ rays, and α and β particles, which may be fatal to humans [8]. Therefore, to prevent the leakage of nuclear fission products, a protective cladding outside the UO_2 fuel block should be provided as the first barrier for nuclear reactor safety [9]. Fig. 1 shows the schematic of the fuel cladding in a nuclear reactor [10]. Rickover *et al.* [11] discovered the advantages of zirconium alloys, which influence the recent decision to use zirconium alloys as fuel cladding. Zirconium and its alloys have a low thermal neutron absorption cross-section, which could reduce the loss of neutrons as they pass through the fuel cladding [12–14]. Additionally, zirconium alloys have good mechanical properties and irradiation effects [15]. The zirconium alloys used in various reactors are shown in Table 1.

Fig. 1. Schematic of a fuel cladding in the nuclear reactor. Reprinted from *J. Nucl. Mater.*, 521, R.B. Adamson, C.E. Coleman, and M. Griffiths, Irradiation creep and growth of zirconium alloys: A critical review, 167-244, Copyright 2019, with permission from Elsevier.

The fuel cladding failure was first discovered in 1963 when General Electric used high-power fuel for testing. The fuel block that expands due to high-power temperature rise squeezes the fuel cladding; this phenomenon is called pellet–cladding interaction (PCI), which causes the failure of

✉ Corresponding authors: Changchun Ge E-mail: ccge@mater.ustb.edu.cn; Yingchun Zhang E-mail: zhang@ustb.edu.cn

Table 1. Summary of zirconium alloys for nuclear fuel claddings

Grade	Alloy composition	Types of reactor	Origin	Refs.
Zr-2	Sn, Fe, Cr, Ni	BWR	America	[16–17]
Zr-4	Sn, Fe, Cr	PWR; LWR	America	[17–18]
ZIRLO	Sn, Nb, Fe	PWR	America; China; Europe	[19–20]
M5	Sn, Nb, O	PWR; RBMK	America; China; Europe	[21–22]
E110	Nb	RBMK	Russia	[23–24]
E125	Nb, O	VVER; RBMK	Russia	[23]
E635	Sn, Nb, Fe	RBMK	Russia	[23–25]
X5A	Sn, Fe, Cr, Nb	PWR	America	[26]
NDA	Sn, Nb, Fe, Cr	PWR	Japan	[27]
N18	Sn, Nb, Fe, Cr	PWR; BWR	China	[28]
N36	Sn, Nb, Fe, Cr	PWR; BWR	China	[28]

Note: BWR—Boiling water reactor; PWR—Pressurized water reactor; LWR—Light water reactor; RBMK—Graphite moderated boiling water reactor; VVER—Water–water energetic reactor.

zirconium alloy cladding [29–30]. Failure events have become frequent since the Canada Deuterium Uranium reactor started operation in 1969. In fact, PCI failure occurred before the widespread use of zirconium alloys as fuel cladding, which indicated that PCI is a common phenomenon during reactor operations [31]. This phenomenon has attracted significant attention. Therefore, it is necessary to understand the stress of fuel claddings during reactor operations. Terrani [32] studied the changes in the diameter of fuel cladding and fuel block as burnup increases. Fig. 2 shows the curve of fuel cladding and pellet diameter with increasing power in the light water reactor. As shown in Fig. 2, the pellet and cladding will undergo thermal expansion when the reactor starts operating. When the burnup is below 20 MWd/kgU, fuel cladding is not generally subjected to hoop stress because a gap still exists between the fuel block and fuel cladding [33–34]. With 20 MWd/kgU, because of the swelling of the pellet and creep-down of fuel cladding, extrusion stress occurs between them, which will increase with fuel consumption.

Several experiments have shown that the failure mode of PCI is stress corrosion cracking (SCC) [35]. Additionally, aggressive fission products, such as I and Cs, will be released with the operation of the reactor. Particularly, iodine has a great influence on zirconium alloy cladding [36]. Zirconium alloy cladding will cause iodine-induced stress corrosion cracking (I-SCC) due to the chemical effect of iodine and the hoop stress on fuel cladding. Research on I-SCC, which has been performed by studying the production conditions and mechanisms, is targeted to prevent significant losses caused by the failure of zirconium alloy cladding. This review summarizes the causes and influencing factors of I-SCC in various zirconium alloy fuel cladding.

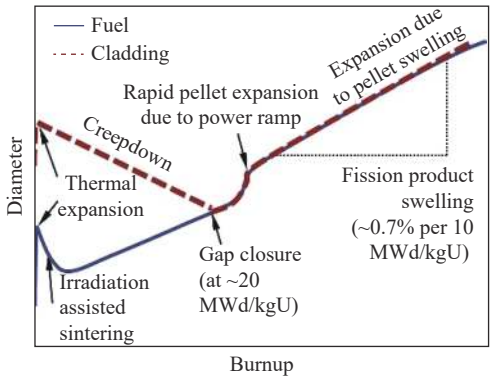

Fig. 2. Curve of the fuel cladding and pellet diameter with increasing power in the light water reactor. Reprinted from *J. Nucl. Mater.*, 501, K.A. Terrani, Accident tolerant fuel cladding development: Promise, status, and challenges, 13-30, Copyright 2018, with permission from Elsevier.

2. Stress corrosion cracking mechanism

2.1. Iodine

The SCC mechanism of zirconium alloy claddings is particularly complicated, which is mainly related to corrosion environment, stress, and materials. Therefore, it is necessary to determine the content and source of iodine in fission products. Gartner and LaVake [37] reported the diffusion of Cs and I from UO_2. Approximately 0.5 g of I-129 was released after a burnup of 30 MWd per kg UO_2 in a 3-kg fuel rod [38]. Fig. 3 shows the production of cesium and iodine during reactor operation [39]. The chemical decomposition

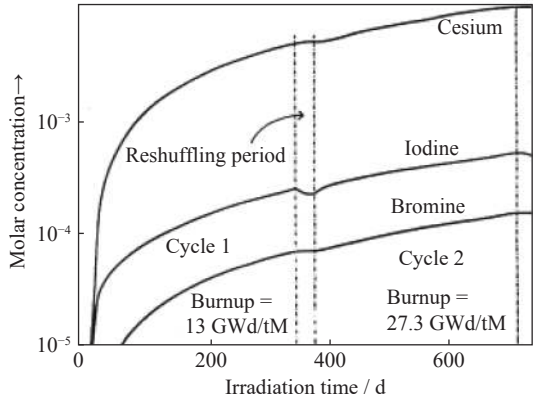

Fig. 3. Production of cesium and iodine in a 17 × 17 fuel rod. Adapted from *J. Nucl. Mater.*, 87, P. Bouffioux, J.V. Vliet, P. Deramaix, and M. Lippens, Potential causes of failures associated with power changes in LWR's, 251-258, Copyright 1979, with permission from Elsevier.

of CsI can produce iodine, but it is mainly from radiation decomposition [40].

Generally, the specific chemical element responsible for SCC in claddings is I, which is considered a pathogenic factor due to its relatively high yield of fission products, diffusibility, and volatility in fuels. There has been controversy about whether iodine promotes SCC alone or with other fission product elements, especially Cs [29]. The argument is sparked by volatility and higher fission product production of Cs compared to that of I. An early investigation claimed that iodine is the most likely corrosive agent because the fracture mode of SCC failure in the laboratory iodine environment closely matches the conditions experienced in a reactor. By contrast, laboratory failure in the Cs environment is not the case.

2.2. Crack initiation

According to Armijo *et al.*'s report [41], high local iodine concentrations were discovered on cladding at the location of particle cracks. Researchers speculated that iodine would probably weaken the bonding force between zirconium atoms and react with zirconium. To verify this assumption, many experiments have been conducted to explore the causes and influencing factors of I-SCC in zirconium alloy claddings [42]. Experimental results have shown that different iodine zirconium compounds will be formed with different amounts of released iodine [43].

Early studies have shown that zirconium and iodine would generate four iodine zirconium compounds: ZrI, ZrI_2, ZrI_3, and ZrI_4 [44]. Cubicciotti *et al.* [45] believed that there might be four reaction processes, in which I_2 and ZrI_4 existed in a gaseous form:

$$Zr + n/2I_2(g) = ZrI_n(s) \quad (1)$$

$$ZrI_n(s) + (m-n)/2I_2(g) = ZrI_m(s),\ m > n \quad (2)$$

$$Zr + n/(4-n)ZrI_4(g) = 4/(4-n)ZrI_n(s) \quad (3)$$

$$ZrI_n(s) + (m-n)/(4-m)ZrI_4(g) = (4-n)/(4-m)ZrI_m(s),\ m > n \quad (4)$$

Peehs *et al.* [36] supplemented the reaction process. A model proposed in the exploration showed that if the iodine pressure was sufficient, then ZrI, ZrI_2, ZrI_3, and ZrI_4 layers were formed in order on the cladding. ZrI_4 is exceptionally volatile at high temperature. These are the current understanding for initiating I-SCC cracks in zirconium alloys. They believed that vapor ZrI_4 converted Zr to solid ZrI on the surface, which would further crack exposure due to the low tensile strength of ZrI. The same conclusion was demonstrated by Gillen *et al.* [46]. The segregation of iodine was first detected at the crack tip using the nanoscale secondary ion mass spectrometry method. The detected iodine is probably from the ZrI mentioned by Peehs *et al.* [36]. However, this result is inconsistent with the previous result by Cox and Haddad [47]. In Cox and Haddad's experiment, no iodine diffusion was detected before the crack tip based on the method of isotope tracer elements [47]. This result may be because the iodine concentration was too low to test using the Rutherford backscattering spectrometry technique. Additionally, these iodine segregation regions corresponded to the zirconium-poor regions in Gillen *et al.*'s experiment [46] and were presumed to be the grain boundaries before the crack tip. The argument that iodine preferentially attacks the grain boundaries has been repeatedly mentioned in the past [48–49].

Aiming at explaining the occurrence of macroscopic cracks, Jezequel *et al.* [50] proposed that pits would be generated on the surface of zirconium alloys and gradually accumulate due to the erosion of iodine. The development of pits is divided into three steps: In the first stage, when the exposure time is not long enough (45 min in their experiments), the surface pits are not obvious. The second stage corresponds to the transition period of pits (24 hours (h) in their experiments). During this period, the pits begin to nucleate, grow, and merge. In the third stage, the pits begin to merge on a large scale. However, Jezequel *et al.* [50] did not explain where the pit started. Before the cracks appeared, pits and pit clusters were generated, which was also confirmed in Park *et al.*'s experimental results [51–52]. Park *et al.* [51] speculated about the reason for the preferential pit nucleation at the grain boundaries on the surface of zirconium alloys. Pits gathered together along the grain boundaries, which contributed to a crack among grain boundaries. Fig. 4 shows the scanning electron microscopy (SEM) images of the surface after I-SCC [50]. Fig. 4 also shows that the pits slowly grow and gather into pit clusters. Fig. 5 shows the SEM images of the fractured cross-section after I-SCC [51]. In Fig. 5, microcracks between the grain boundaries appear on the surface away from the fracture.

2.3. Crack propagation

Recently, grain-boundary pitting coalescence (GBPC) and pitting-assisted slip cleavage (PASC) models have been proposed to summarize the mechanism of I-SCC crack initiation and propagation on the surface of zirconium alloys. The I-SCC failure can be described in four stages: (i) crack initiation, (ii) localized intergranular (IG) crack growth, (iii) transgranular (TG) crack propagation, and (iv) final failure [49]. Fig. 6 shows a diagram of the breakage of GBPC and PASC models [51]. The microcracks generated along the grain boundary (GB) will contribute to I-SCC cracks growing by an IG mode in the early stage of cracking. Farina *et al.* [53] believed that IG corrosion is the prerequisite for SCC to occur. However, in different iodine environments, the factors affecting IG corrosion are different. Zirconium atoms are transferred through the Van Arkel vapor transport mechanism in an iodine vapor environment [54]. Conversely, in iodine solutions, researchers believe that IG corrosion is controlled by the diffusion of active materials to the crack tip [55]. The details will be unfolded in Section 3.1.

When the crack growth reaches a critical point, some IG cracks will change to the TG mode and become a mixed propagation mode of IG and TG. In the mixed propagation mode, TG cracks can pass through one grain but cannot further penetrate into the adjacent grains, so it changes its direc-

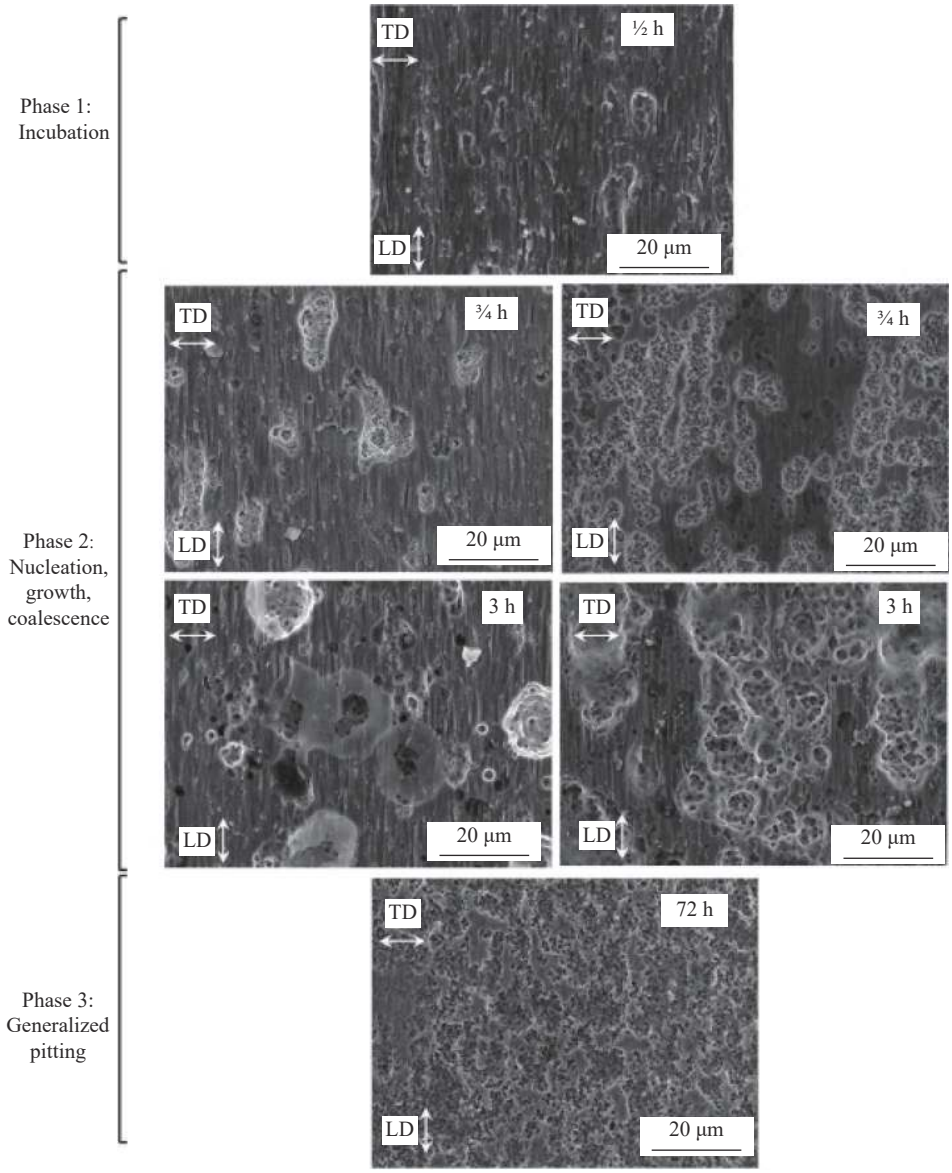

Fig. 4. SEM images of the surface after induced-stress corrosion cracking. TD stands for transversal direction; LD stands for longitudinal direction. Reprinted from *J. Nucl. Mater.*, 499, T. Jezequel, Q. Auzoux, D.L. Boulch, M. Bono, E. Andrieu, C. Blanc, V. Chabretou, N. Mozzani, and M. Rautenberg, Stress corrosion crack initiation of Zircaloy-4 cladding tubes in an iodine vapor environment during creep, relaxation, and constant strain rate tests, 641-651, Copyright 2018, with permission from Elsevier.

tion along the grain boundary with the appearance of IG cracks along several grains. A large number of experiments show that TG cracks in zirconium alloys will propagate parallel to the base surface [56–57]. Fig. 7 shows the SEM fracture diagram of the mixed propagation mode of IG and TG in Zircaloy-4 [51]. Park *et al.* [51] proposed three main situations for the emergence of the hybrid model. In the first case, when the pits and related microcracks are arranged on the line of the plane of the cleavage habits of the grains, the cleavage cracks will occur at low-stress intensity. By contrast, the stress intensity factor (K_I) value increases as the crack depth becomes significant, and when the K_I value is high enough, cleavage cracks occur only through nanoscale pittings. In the second case, if the habitual plane of adjacent grains and TG crack grains are not parallel and the stress intensity is not high enough, then the cleavage will not extend to the adjacent grains, and the cleavage will stop at the grain boundary. In the third case, the next cleavage crack will be induced due to the continuous accumulation of IG cracks.

Furthermore, crack growth develops to follow the TG propagation mode. Cracks propagate through cleavage-like TG cracks that pass through one grain to the adjacent grain without changing their direction. When the crack depth is deep enough, due to the high-stress intensity at the crack tip, cleavage cracking will occur without PASC or selective crystal planes. Meanwhile, the crack growth rate at this stage is very high because the cracks caused by TG present continuous cleavage fractures.

Finally, there is the ductile (DUC) fracture zone, as shown in Fig. 8 [48]. The I-SCC fracture usually refers to IG and TG fractures. However, the DUC fracture can occur in an environment where there is no corrosive medium, as long as the stress is extremely large [58–60]. Therefore, the DUC fracture part is out of the scope of this article.

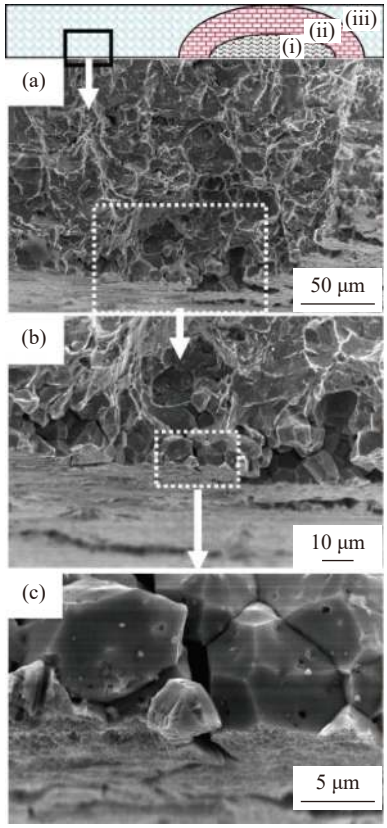

Fig. 5. SEM images of the fractured cross-section after induced-stress corrosion cracking: (a) 500×, (b) 1000×, and (c) 5000×. Reprinted from *J. Nucl. Mater.*, 376, S.Y. Park, J.H. Kim, M.H. Lee, and Y.H. Jeong, Effects of the microstructure and alloying elements on the iodine-induced stress-corrosion cracking behavior of nuclear fuel claddings, 98-107, Copyright 2008, with permission from Elsevier.

3. Influencing factors of induced-stress corrosion cracking cracking

3.1. Iodine environment

As mentioned earlier, the iodine environment has a great influence on the corrosion and cracking of the zirconium alloy fuel claddings. Currently, the corrosive environment in which stress corrosion occurs in laboratory research can be divided into the iodine vapor environment and the iodine solution environment. Cox and Wood proved [61] that I-SCC is the condition closest to the state of use in a gaseous iodine environment of approximately 300°C. However, many studies regarding I-SCC testing in iodine solution are conducted at room temperature because experimental equipment is quite vulnerable in the iodine vapor environment, which is also valuable. In the iodine vapor environment, the influence of partial iodine pressure on I-SCC is mainly studied, while in the iodine solution environment, the influences of different solutions and iodine concentration are mainly studied.

Whether the experiments are performed in iodine vapor or in an iodine solution, the consistent result is that an increase in iodine concentration can increase the rate of crack growth. The higher the iodine concentration is, the shorter the failure time is when the other conditions are the same. Additionally, a low-stress intensity factor is required for crack initiation with a high iodine concentration [62]. Serres *et al.* [63] compared the test results in an iodized methanol solution with different iodine concentrations, and the results showed that when the iodine concentration was increased to 10 times, the crack growth rate could be accelerated to 2.6 times. They concluded that when the K_I value is constant, the increase in the iodine concentration will boost the growth rate of cracks. It is assumed that the IG fracture will be affected by the iodine concentration. Using the fractal observation method, Gillen *et al.* [64] came to a positive conclusion that the rate of crack growth increases with the iodine concentration. The proportion of TG fracture area will decrease, whereas the IG fracture and DUC fracture area will increase because of the increase in iodine concentration. Fournier *et al.* [62] found that at an iodine concentration of 6×10^{-6} g/g, crack initiation occurred at a macroscopic plastic strain of 0.5%, while no significant crack initiation was observed at an iodine con-

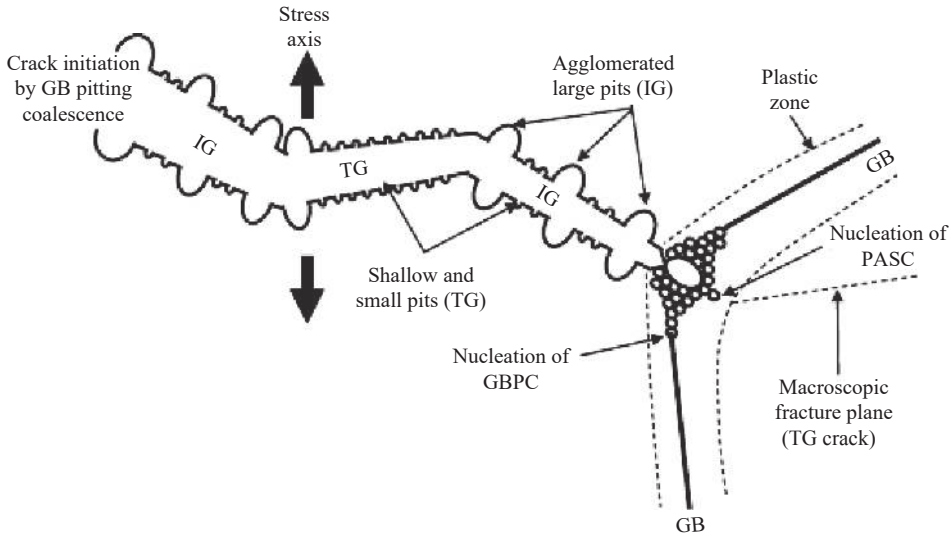

Fig. 6. Schematic of the GBPC and PASC crack growth models. Reprinted from *J. Nucl. Mater.*, 376, S.Y. Park, J.H. Kim, M.H. Lee, and Y.H. Jeong, Effects of the microstructure and alloying elements on the iodine-induced stress-corrosion cracking behavior of nuclear fuel claddings, 98-107, Copyright 2008, with permission from Elsevier.

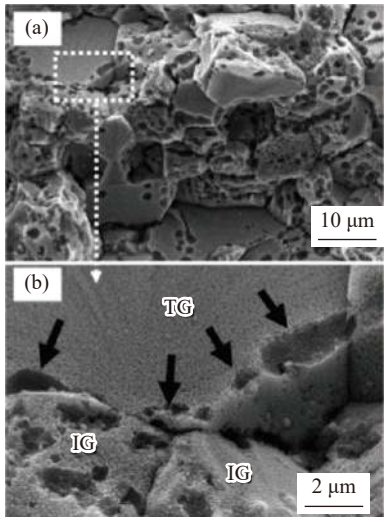

Fig. 7. (a) SEM fractographs of the IG and TG mixed propagation modes in Zircaloy-4; (b) enlarged micrograph of the dotted area in (a). Reprinted from *J. Nucl. Mater.*, 376, S.Y. Park, J.H. Kim, M.H. Lee, and Y.H. Jeong, Effects of the microstructure and alloying elements on the iodine-induced stress-corrosion cracking behavior of nuclear fuel claddings, 98-107, Copyright 2008, with permission from Elsevier.

centration of 10^{-6} g/g. This finding manifests that the intensity factor required for crack propagation is reduced because of the high iodine concentration. It is agreed that excessive iodine would react with zirconium to form complex zirconium iodide, which is the cause of crack initiation. More iodine present will result in more Zr attacked, and consequently, more complex zirconium iodide will be formed, and the corrosion rate will increase [65]. However, there is a saturation value when the iodine concentration rises. After the saturation value is exceeded, the iodine concentration will no longer affect the failure time [66–67]. Recently, Gillen *et al.* [64] studied compression tests of C-rings with iodine concentrations between 0.1 and 20 mg/cm^3 in iodine ethanol solutions. Fig. 9 shows the failure time of cold working (CW) and recrystallized (RX) ZIRLO in iodized ethanol solutions with different iodine concentrations after C-ring compression tests. They confirmed once again that when the iodine concentration is greater than 1 mg/cm^3, the failure time will no longer decrease as the iodine concentration increases. Although the saturation values obtained from various experiments are slightly different, the magnitudes are the same. When iodine reaches a saturated state, there is enough iodine locally, and the amount of zirconium available is nearly consumed. The amount of zirconium is the same, so further increasing the iodine concentration will not cause more reactions.

In the early stage of crack propagation (IG propagation stage), many scholars believe that the crack propagation mechanism in iodine vapor and iodine solution varies [68] because alcohol iodine has more extraordinary corrosive properties than gaseous iodine [69]. Zirconium atoms are transferred following the Van Arkel vapor transport mechanism in the iodine vapor environment [54]. ZrI, ZrI_2, ZrI_3, and ZrI_4 layers are formed in order on the cladding when the iodine pressure is sufficient. ZrI_4 is a volatile solid that will then diffuse as a vapor from the crack tip to its mouth, thus removing Zr and deepening the crack. Conversely, many studies have shown that the stress-assisted dissolution–adsorption mechanism may cause the IG propagation stage in the iodine solution environment [70]. The IG attack occurs through a chemical dissolution of the grain boundaries, assisted by the applied stress. Zirconium is adsorbed by the free iodide ions in the solution to form zirconium-iodide compounds. However, the zirconium-iodide compounds do not exist as gases because of the low temperature. Moreover, the diffusion of the active species (iodine-alcohol complex) probably controls IG cracking [71]. Generally, whether in the environment of iodine vapor or iodine solution, when the stress intensity factor, K_I, reaches a critical value, the IG–TG transition will occur.

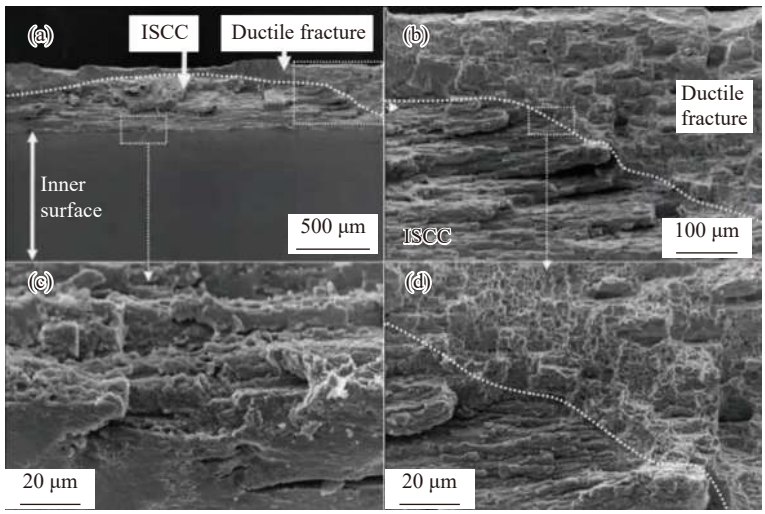

Fig. 8. (a) SEM image of I-SCC and ductile fractures; (b, c) enlarged micrographs of the dotted areas in (a); (d) enlarged micrograph of the dotted area in (b). Reprinted from *J. Nucl. Mater.*, 372, S.Y. Park, J.H. Kim, M.H. Lee, and Y.H. Jeong, Stress-corrosion crack initiation and propagation behavior of Zircaloy-4 cladding under an iodine environment, 293-303, Copyright 2008, with permission from Elsevier.

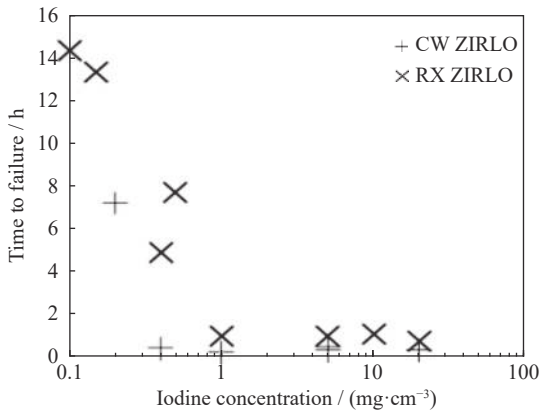

Fig. 9. Failure time of CW and RX ZIRLO in an iodized ethanol solution with different iodine concentrations after C-ring compression tests. Reprinted from *J. Nucl. Mater.*, 539, C. Gillen, A. Garner, C. Anghel, and P. Frankel, Investigating iodine-induced stress corrosion cracking of zirconium alloys using quantitative fractography, 152272, Copyright 2020, with permission from Elsevier.

3.2. Temperature

Azevedo [72] proposed that, under normal conditions, the temperature of the inner diameter of the cladding can reach 300–400°C when the reactor is in operation. However, in the event of a pellet–cladding physical interaction, the temperature of the cladding can reach 1000°C. Therefore, to study the effect of temperature on iodine-induced SCC, the temperature range is mostly set between 300 and 400°C (iodine vapor environment). For the iodine solution environment, the temperature is usually between 10 and 100°C. In the I-SCC process of zirconium alloys, the rise in temperature can lead to three consequences. The first one is the reduction in the strength of the material and the increase in its toughness. The second one is the promotion of stress release at the crack tip. The third one is the acceleration of the corrosive effect of iodine on zirconium alloys. A large number of experiments have shown that the stress intensity factor K_I will decrease with the increase in temperature [57,73]. When the temperature rises in the crack initiation stage, the stress at the crack tip is likely to release due to local plastic deformation, which makes the diffusion of iodine along the grain boundary easy, so the required cracking stress becomes low. Moreover, the failure time of zirconium alloys will be shortened due to the increase in temperature, which has been confirmed in many kinds of research. Jezequel *et al.* [50] studied the I-SCC behavior of zirconium alloys in iodine vapor environments from 320 to 380°C. They also agreed that an increase in temperature will decrease failure time and increase failure strain. They found that the increase in temperature will increase the minimum strain at failure. When the temperature increased from 320 to 380°C, the minimum failure strain increased from 0.4% to 1%. However, the threshold stress would not change when the temperature rose (240 MPa in this experiment). This finding is consistent with previous ones [74–75]. The authors believe that the threshold stress is related to the strength of the material itself. Moreover, temperature changes have no obvious effect on pitting corrosion behavior. Sanchez *et al.* [76] explored the failure of zirconium alloys in iodized butanol and iodized pentanol solutions at temperatures ranging from 20 to 90°C. Fig. 10 shows the failure time crack propagation rate (cpr) diagrams of zirconium alloys at different temperatures. In Fig. 10, the failure time and cpr decrease as the temperature increases from 20 to 90°C. The increase in temperature will increase the total length of the brittle area (IG plus TG).

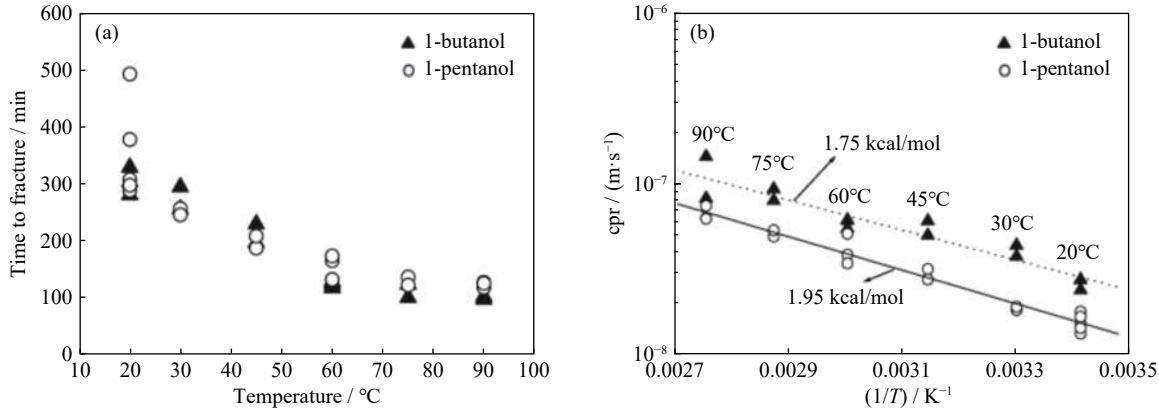

Fig. 10. (a) Failure time and (b) cpr diagrams of zirconium alloys at different temperatures. Reprinted from *Corros. Sci.*, 49, A.V.G. Sanchez, S.B. Farina, and G.S. Duffó, Effect of temperature on the stress corrosion cracking of Zircaloy-4 in iodine alcoholic solutions, 3112-3117, Copyright 2007, with permission from Elsevier.

3.3. Microstructure

After each CW of zirconium alloy plate or pipe, it needs to restore its ductility through annealing treatment [77]. RX zirconium alloy is usually annealed at 550 to 669°C, and its grain morphology is equiaxed. Additionally, there is a stress relief (SR) state, which avoids complete recrystallization by lowering the final annealing temperature [78]. The morphology of the grains presents the characteristics of long grains and a high density of dislocations. Gillen *et al.* [46] studied the I-SCC behavior of zirconium alloys under CW and RX conditions. Fig. 11 shows the electron backscatter diffraction images of CW and RX ZIRLO cladding tubes. The CW ma-

terial exhibits typically elongated grains with an approximate dimension of 2 μm × 10 μm. The RX process produces an equiaxed microstructure with grains of ~2 μm diameter. This experiment shows that the direction of crack propagation is different on CW and RX materials from the perspective of macroscopic cracks. Fig. 12 shows optical micrographs of typical cracks in RX and CW ZIRLO. Cracks mainly propagate in the radial direction on the RX sample. In the CW sample, it first propagates in the radial direction, then changes to the tangent direction of 30°, and finally splits a crack toward 130° to the tangent line. There are more linear and fewer cracks in the CW sample than in the RX sample at the initial stage. However, CW cracks tend to have more tangential crack paths macroscopically. This condition is probably because the macroscopic crack direction generally follows the shortest and highest stressed route [79].

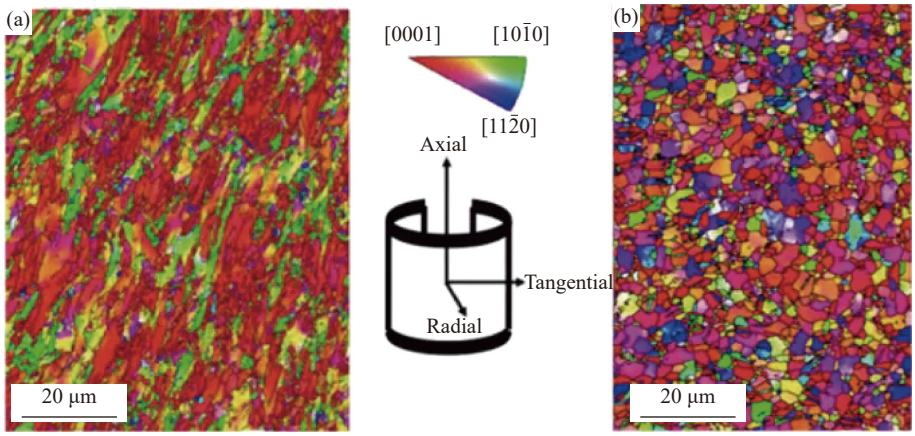

Fig. 11. Electron backscatter diffraction images of ZIRLO cladding tubes: (a) CW and (b) RX [46].

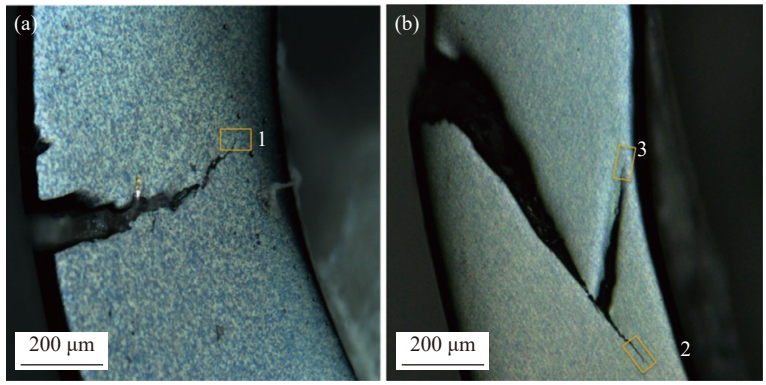

Fig. 12. Optical micrographs of typical cracks in (a) RX and (b) CW ZIRLO [46].

Fig. 13 shows the schematic diagrams of pits formed on the surfaces of SR and RX grains [48]. In Fig. 13, the SR material exhibits typically elongated grains, which are similar in shape to CW grains. During the I-SCC cracking, grain shape and cleavage habit plane play an important role in grain cracking. Park *et al.* [48,51] found that the failure time of the RX sample was 80 times that of the SR sample. For Zircaloy-4, RX can increase the resistance of I-SCC. Its K_I is 4.8 MPa·m$^{0.5}$, and SR's K_I is 3.3 MPa·m$^{0.5}$. However, for alloy ZIRLO, there is no difference in the results of RX and SR samples.

The performance of fracture varies with the shape of the crystal grains. Fig. 14 shows the SEM images of IG, TG, and DUC fractures of zirconium alloys with CW [64], SR [51], and RX [64] grains. Fig. 14 shows the features of similar size and shape to the grains in the IG fracture for CW and SR materials. In the TG fracture region, perpendicular fluting steps interrupt the stepped cracking with cleavage planes. For the RX material, the features of size and shape to the grains in the IG fracture are similar to those of the CW and SR materials. In the TG fracture region, the fracture exhibits flat TG crack-

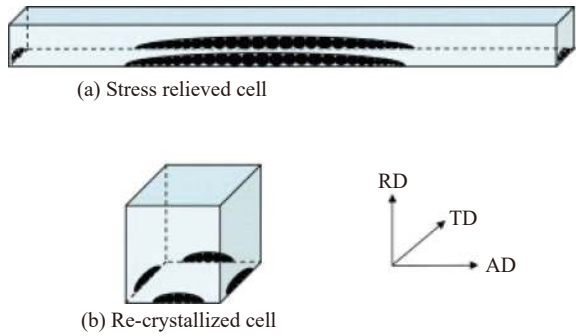

Fig. 13. Schematic of pits formed on the surface of (a) SR and (b) RX grains. RD stands for radial direction; TD stands for tangential direction; AD stands for axial direction. Reprinted from *J. Nucl. Mater.*, 372, S.Y. Park, J.H. Kim, M.H. Lee, and Y.H. Jeong, Stress-corrosion crack initiation and propagation behavior of Zircaloy-4 cladding under an iodine environment, 293-303, Copyright 2008, with permission from Elsevier.

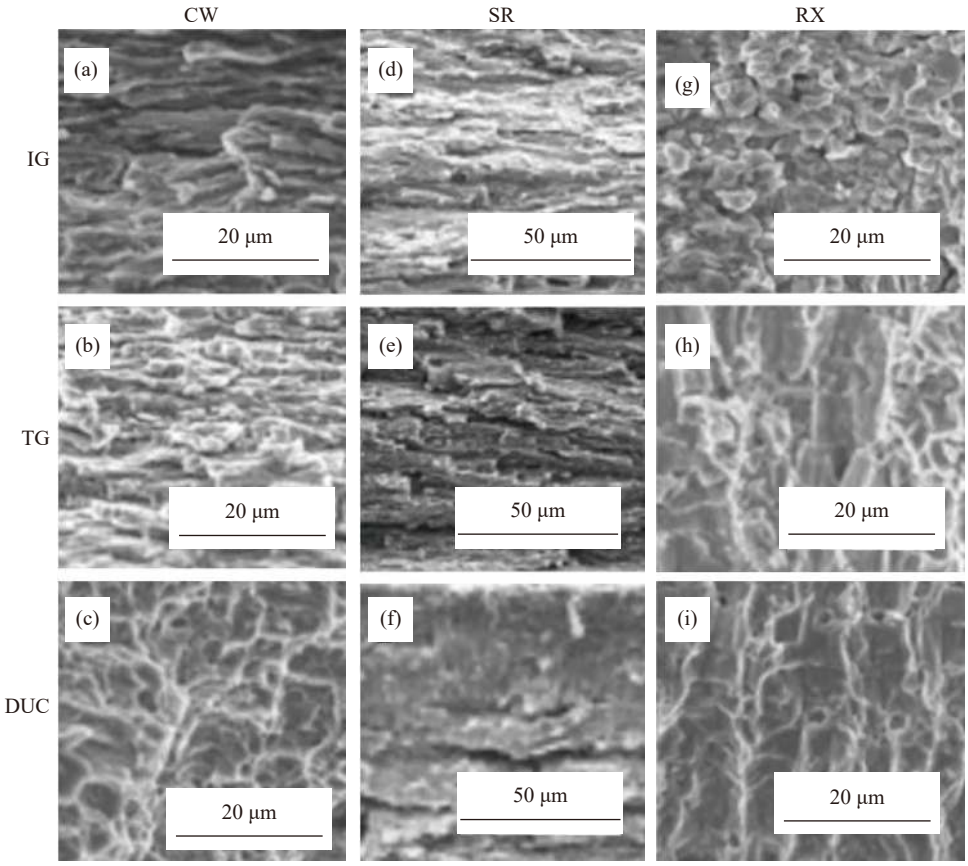

Fig. 14. SEM images of the IG, TG, and DUC fractures of zirconium alloys with (a–c) CW, (d–f) SR, and (g–i) RX grains. (a–c) and (g–i): Reprinted from *J. Nucl. Mater.*, 539, C. Gillen, A. Garner, C. Anghel, and P. Frankel, Investigating iodine-induced stress corrosion cracking of zirconium alloys using quantitative fractography, 152272, Copyright 2020, with permission from Elsevier; (d–f): Reprinted from *J. Nucl. Mater.*, 376, S.Y. Park, J.H. Kim, M.H. Lee, and Y.H. Jeong, Effects of the microstructure and alloying elements on the iodine-induced stress-corrosion cracking behavior of nuclear fuel claddings, 98-107, Copyright 2008, with permission from Elsevier.

ing of cleavage without fluting. In CW, SR, and RX materials, spherical microvoids are exhibited in the DUC region.

3.4. Alloying elements

Generally, among the alloying elements Sn, Ni, Nb, Fe, Cr, and O, oxygen is regarded as an alloying element rather than an impurity. Previous studies have shown that various zirconium alloys contain different elements, which will lead to different material strengths. However, it has not been observed that the types and contents of these elements have a significant impact on I-SCC mechanics [80]. However, recent studies have found different conclusions, suggesting that alloying elements have an influence on the fracture of I-SCC. In 2008, the Park group [51] compared the I-SCC behavior of Zircaloy-4 and ZIRLO alloys. They found that the GB pitting corrosion resistance of Zircaloy-4 is lower than that of alloy ZIRLO because according to the SEM fractographs, many pits severely attack the surface of the IG region in the Zircaloy-4 alloy, and there are only small pits (nanoscale) on the surfaces of IG and TG regions in the ZIRLO alloy. Moreover, the I-SCC performances of the two zirconium alloys after heat treatment are different. Specifically, the K_I in the SR and RX states of Zircaloy-4 are 3.3 and 4.8 MPa·m$^{0.5}$, respectively, but there is no difference between the K_I values in the SR and RX states of the ZIRLO alloy. Additionally, experiments have shown that adding oxygen can form interstitial solid solutions and increase the yield strength of zirconium alloys. Traces of Fe, Cr, and Ni in Zircaloy occur as precipitated compounds [81]. The iodine reaction rates with Fe and Ni are much higher than that with Zr at the in-reactor temperatures, so precipitated phases will react with excessive iodine to form metal iodides and thus supply ZrI_4 locally.

Up to now, the studies on zirconium alloys are not comprehensive enough. Li *et al.* [82] prepared pure Zr coatings on the surface of the ZIRLO alloy. They found that the I-SCC resistance of the ZIRLO alloy was enhanced by Zr coatings. Specifically, Zr coatings could reduce the diffusion rate of iodine from 3.258×10^{-12} to 0.175×10^{-12} m^2/s. Therefore, alloy elements certainly have an influence on the I-SCC behavior of zirconium alloys.

3.5. Oxide layer

Zirconium oxides are easy to form by reacting with oxygen. A natural oxide with a nanometer thickness is easy to form on the surface of zirconium alloy cladding. Therefore, considerable research has focused on whether oxides can resist I-SCC. Mattas *et al.* [83] reported that a layer of thick oxide can slow down the occurrence of I-SCC because of the

compressive stress due to the volume (Pilling–Bedworth) ratio of oxide to metal for ZrO_2. I-SCC occurred after the oxide was mechanically breached. The loss of ductility at the fracture of Zircaloy-4 is more significant when iodine is admitted in a vacuum than in the air. However, an oxide film should not be relied on as a long-term protection method against I-SCC. When the oxide film is not thick enough, iodine can easily penetrate the oxide film and react with zirconium. Additionally, pitting corrosion was found on the surface of the zirconium alloy [50]. Based on observations reported in the literature [84–85], the following pitting mechanism is proposed. Fig. 15 illustrates the proposed mechanism [50]. First, the oxide film is produced because of the oxygen reacting between oxygen and zirconium. Iodine can penetrate the oxide layer and react with zirconium to form gaseous zirconium tetraiodide (ZrI_4). Then, gaseous zirconium tetraiodide makes the gas pressure too high to break the oxide layer. Eventually, the entire oxide layer flakes off, leaving the entire zirconium surface covered in pits, which corresponds to the generalized pitting phase previously mentioned.

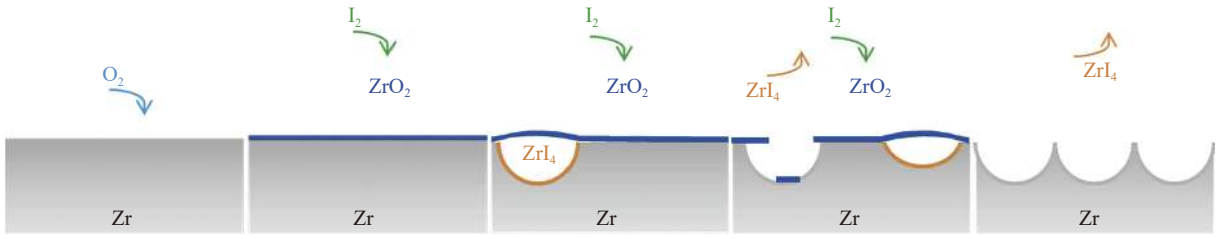

Fig. 15. Proposed mechanism for the pitting of the Zircaloy-4 surface exposed to iodine vapor. Reprinted from *J. Nucl. Mater.*, 499, T. Jezequel, Q. Auzoux, D.L. Boulch, M. Bono, E. Andrieu, C. Blanc, V. Chabretou, N. Mozzani, and M. Rautenberg, Stress corrosion crack initiation of Zircaloy-4 cladding tubes in an iodine vapor environment during creep, relaxation, and constant strain rate tests, 641-651, Copyright 2018, with permission from Elsevier.

4. Conclusions and prospects

The PCI failure occurs between the zirconium alloy cladding and fuel block, which will cause huge losses. I-SCC will occur on the zirconium alloy cladding under the chemical action of the fission product iodine. In this review, the mechanism of I-SCC among various zirconium alloy fuel cladding is summarized. Micropits are formed on the surface of the zirconium alloy due to the reaction between iodine and zirconium, and then small pits gradually gather to form pit clusters. Cracks are easily generated in the pit clusters and propagate along the grain boundary. After a critical point, the crack will transform into TG direction propagation. As the crack develops, it ends with a DUC fracture. Iodine will affect the initiation of I-SCC cracks and plays an important role in IG cracking.

We also summarize various factors that may affect I-SCC. The specific cracking conditions depend on various factors, such as iodine concentration, temperature, microstructure, alloying elements, and oxide layer. Specifically, the time for the specimens to break will increase due to the increase in iodine concentration, whether in an iodine solution or an iodine vapor environment. The higher the iodine concentration is, the lower the stress intensity factor required for crack initiation. Additionally, the proportion of the TG fracture area will shrink, whereas the IG and DUC fracture areas will enlarge because of the increase in iodine concentration. The stress intensity factor K_I will decrease with the increase in temperature, which will accelerate the corrosive effect of iodine on zirconium alloys. Microstructure also affects the development of I-SCC. In a nutshell, equiaxed crystals are more resistant to I-SCC than long strips. Until now, research on zirconium alloy is not comprehensive enough, but alloying elements certainly have a particular influence on the I-SCC behavior of zirconium alloys. The oxide layer is chemically resistant to iodine corrosion, but it is likely to crack under stress, resulting in pits and stress concentration, which is unideal for the effect of resisting I-SCC. Hopefully, the summary on the impact of these factors on I-SCC will provide a reference for the effective prevention of I-SCC in the future.

Based on this review, we recommend two research aspects for resistance to I-SCC. One is to adjust the element types and proportions of zirconium alloys. The other is to find coating materials that can resist I-SCC on the surface of zirconium alloys. Because the environment inside the reactor is uncontrollable, more attention can be paid to material properties, such as alloying elements, microstructure, and surface treatment, to improve the I-SCC resistance of zirconium alloys.

Acknowledgements

This study was supported by the National MCF Energy R&D Program (No. 2019YFE03130002) and the Research Program of Development Strategy of the Chinese Academy of Sciences (No. XK2019JSA001).

Conflict of Interest

The authors declare that they have no known competing interests or personal relationships that could have appeared to influence the work reported in this paper.

References

[1] M.M. Abu-Khader, Recent advances in nuclear power: A review, *Prog. Nucl. Energy*, 51(2009), No. 2, p. 225.
[2] C.T. Whitman, The case for nuclear power, *Business Week*,

2007, No. 4050, p. 102.
[3] J.P. Howe, The beginning of nuclear materials: Studies of corrosion and cladding, *J. Nucl. Mater.*, 100(1981), No. 1-3, p. 36.
[4] R.L.S. Martin, *Environmental Emissions from Energy Technology Systems: The Total Fuel Cycle*, US Department of Energy, Washington, 1989 [2021-08-10]. https://doi.org/10.2172/860715
[5] E.I. Grishanin, The role of chemical reactions in the Chernobyl accident, *Phys. Atom. Nuclei*, 73(2010), No. 14, p. 2296.
[6] F. Tanabe, Analyses of core melt and re-melt in the Fukushima Daiichi nuclear reactors, *J. Nucl. Sci. Technol.*, 49(2012), No. 1, p. 18.
[7] G. Steinhauser, A. Brandl, and T.E. Johnson, Comparison of the Chernobyl and Fukushima nuclear accidents: A review of the environmental impacts, *Sci. Total. Environ.*, 470-471(2014), p. 800.
[8] S. Uchida, H. Karasawa, C. Kino, M. Pellegrini, M. Naitoh, and M. Ohsaka, An approach toward evaluation of long-term fission product distributions in the Fukushima Daiichi nuclear power plant after the severe accident, *Nucl. Eng. Des.*, 380(2021), art. No. 111256.
[9] Z. Karoutas, J. Brown, A. Atwood, L. Hallstadius, E. Lahoda, S. Ray, and J. Bradfute, The maturing of nuclear fuel: Past to accident tolerant fuel, *Prog. Nucl. Energy*, 102(2018), p. 68.
[10] R.B. Adamson, C.E. Coleman, and M. Griffiths, Irradiation creep and growth of zirconium alloys: A critical review, *J. Nucl. Mater.*, 521(2019), p. 167.
[11] H.G. Rickover, L.D. Geiger, and B. Lustman, *History of The Development of Zirconium Alloys for Use in Nuclear Reactors*, US Energy Research and Development Administration, Washington, 1975 [2021-08-01]. https://doi.org/10.2172/4240391
[12] H. Pomerance, Thermal neutron capture cross sections, *Phys. Rev.*, 88(1952), No. 2, p. 412.
[13] L. Xu, Y. Xiao, A. van Sandwijk, Q. Xu, and Y. Yang, Production of nuclear grade zirconium: A review, *J. Nucl. Mater.*, 466(2015), p. 21.
[14] G. Pan, C.J. Long, A.M. Garde, A.R. Atwood, J.P. Foster, R.J. Comstock, L. Hallstadius, D.L. Nuhfer, and R. Baranwal, Advanced material for PWR application: AXIOM™ cladding, [in] *Proceedings of International Conference on Light Water Reactor Fuel Performance*, Orlando, Florida, 2010.
[15] K.A. Terrani, S.J. Zinkle, and L.L. Snead, Advanced oxidation-resistant iron-based alloys for LWR fuel cladding, *J. Nucl. Mater.*, 448(2014), No. 1-3, p. 420.
[16] S. Kass. The development of the zircaloys, [in] W.K. Anderson, ed., *Corrosion of Zirconium Alloys*, the American Society for Testing and Materials, Philadelphia, 1964, p. 3.
[17] C.L. Whitmarsh, *Review of Zircaloy-2 and Zircaloy-4 Properties Relevant to N.S. Savannah Reactor Design*, Oak Ridge National Laboratory, Oak Ridge, 1962 [2021-08-20]. https://doi.org/10.2172/4827123
[18] A.M. Garde, S.R. Pati, M.A. Krammen, G.P. Smith, and R.K. Endter, Corrosion behavior of Zircaloy-4 cladding with varying tin content in high-temperature pressurized water reactors, [in] *Zirconium in the Nuclear Industry: Tenth International Symposium*, Baltimore, MD, 1994.
[19] G.P. Sabol, G.R. Kilp, M.G. Balfour, and E. Roberts, Development of a cladding alloy for high burnup, [in] *Zirconium in the Nuclear Industry: Eighth International Symposium*, San Diego, 1988.
[20] G.P. Sabol, R.J. Comstock, R.A. Weiner, P. Larouere, and R.N. Stanutz, In-reactor corrosion performance of ZIRLO™ and Zircaloy-4, [in] *Zirconium in the Nuclear Industry: Tenth International Symposium*, Baltimore, MD, 1994.
[21] S. Doriot, D. Gilbon, J.L. Béchade, M.H. Mathon, L. Legras, and J.P. Mardon, Microstructural stability of M5™ alloy irradiated up to high neutron fluences, [in] *Zirconium in the Nuclear Industry: Fourteenth International Symposium*, Stockholm, 2005.
[22] J.P. Mardon, G.L. Garner, and P.B. Hoffmann, M5® a breakthrough in Zr alloy, [in] *Proceedings of International Conference on Light Water Reactor Fuel Performance*, Orlando, Florida, 2010.
[23] V. Novikov, V. Markelov, A. Gusev, A. Malgin, A. Kabanov, and Y. Pimenov, Some results on the properties investigations of zirconium alloys for VVER-1000 fuel cladding, [in] *9th International Conference on WWER Fuel Performance, Modelling and Experimental Support*, Helena Resort, 2011.
[24] A.V. Nikulina, Zirconium alloys in nuclear power engineering, *Met. Sci. Heat Treat.*, 46(2004), No. 11-12, p. 458.
[25] A.V. Nikulina, V.A. Markelov, M.M. Peregud, Y.K. Bibilashvili, V.A. Kotrekhov, A.F. Lositsky, N.V. Kuzmenko, Y.P. Shevnin, V.K. Shamardin, G.P. Kobylyansky, and A.E. Novoselov, Zirconium alloy E635 as a material for fuel rod cladding and other components of VVER and RBMK cores, [in] *Zirconium in the Nuclear Industry: Eleventh International Symposium*, Garmisch-Partenkirchen, 1996.
[26] A.M. Garde, R.J. Comstock, G. Pan, R. Baranwal, L. Hallstadius, T. Cook, and F. Carrera, Advanced zirconium alloy for PWR application, [in] *Zirconium in the Nuclear Industry: 16th International Symposium*, Chengdu, 2010.
[27] F. Garzarolli, P. Rudling, and C. Patterson, *Performance Evaluation of New Advanced Zr Alloys for PWRs/VVER*, Advanced Nuclear Technology International, Mölnlycke, 2011.
[28] W.J. Zhao, B.X. Zhou, Z. Miao, Q. Peng, Y.R. Jiang, H.M. Jiang, H. Pang, C. Li, Y. Gou, X.W. Yu, S.J. Xue, H.T. Chen, Y.Z. Liu, J.H. Peng, and S.Q. Zhao, Development of advanced zirconium alloys used in Chinese nuclear industry, [in] *The 13th International Conference on Nuclear Engineering*, Beijing, 2005.
[29] B. Cox, Pellet-clad interaction (PCI) failures of zirconium alloy fuel cladding—A review, *J. Nucl. Mater.*, 172(1990), No. 3, p. 249.
[30] J.S. Cheon, Y.H. Koo, B.H. Lee, J.Y. Oh, and D.S. Sohn, Modelling of a pellet–clad mechanical interaction in LWR fuel by considering gaseous swelling, [in] *Proceedings of the Seminar on Pellet–clad Interaction in Water Reactor Fuels*, Aix-en-Provence, 2004, p. 191.
[31] B.J. Lewis, W.T. Thompson, M.R. Kleczek, K. Shaheen, M. Juhas, and F.C. Iglesias, Modelling of iodine-induced stress corrosion cracking in CANDU fuel, *J. Nucl. Mater.*, 408(2011), No. 3, p. 209.
[32] K.A. Terrani, Accident tolerant fuel cladding development: Promise, status, and challenges, *J. Nucl. Mater.*, 501(2018), p. 13.
[33] J.J. Serna, P. Tolonen, S. Abeta, S. Watanabe, Y. Kosaka, T. Sendo, and P. Gonzalez, Experimental observations on fuel pellet performance at high burnup, *J. Nucl. Sci. Technol.*, 43(2006), No. 9, p. 1045.
[34] M.H.A. Piro, D. Sunderland, S. Livingstone, J. Sercombe, R.W. Revie, A. Quastel, K.A. Terrani, and C. Judge, Pellet–clad interaction behavior in zirconium alloy fuel cladding, *Compr. Nucl. Mater.*, 2(2020), p. 248.
[35] K. Maeda, Ceramic fuel–cladding interaction, *Compr. Nucl. Mater.*, 3(2012), p. 443.
[36] M. Peehs, F. Garzarolli, R. Hahn, and E. Steinberg, Diskussion möglicher mechanismen von PCI-defekten, *J. Nucl. Mater.*, 87(1979), No. 2-3, p. 274.
[37] M. Gaertner and J.C. LaVake, Power ramp testing and non-destructive post-irradiation examinations of high burnup PWR fuel rods, [in] *Proceedings of the Specialists' Meeting on Pellet Cladding Interaction in Water Reactor Fuel*, Seattle, 1983.
[38] B. van der Schaaf, Fracture of Zircaloy-2 in an environment containing iodine, [in] *Symposium on Zirconium in Nuclear Ap-*

plication, Portland, 1973.
[39] P. Bouffioux, J.V. Vliet, P. Deramaix, and M. Lippens, Potential causes of failures associated with power changes in LWR's, *J. Nucl. Mater.*, 87(1979), No. 2-3, p. 251.
[40] K. Konashi, T. Yato, and H. Kaneko, Radiation effect on partial pressure of fission product iodine, *J. Nucl. Mater.*, 116(1983), No. 1, p. 86.
[41] J.S. Armijo, L.F. Coffin, and H.S. Rosenbaum, Development of zirconium-barrier fuel cladding, [in] *Zirconium in the Nuclear Industry: Tenth International Symposium*, Baltimore, MD, 1994.
[42] A. Garlick and P.D. Wolfenden, Fracture of zirconium alloys in iodine vapour, *J. Nucl. Mater.*, 41(1971), No. 3, p. 274.
[43] P. Hofmann and J. Spino, Determination of the critical iodine concentration for stress corrosion cracking failure of Zircaloy-4 tubing between 500 and 900°C, *J. Nucl. Mater.*, 107(1982), No. 2-3, p. 297.
[44] O. Götzmann, Thermochemical evaluation of PCI failures in LWR fuel pins, *J. Nucl. Mater.*, 107(1982), No. 2-3, p. 185.
[45] D. Cubicciotti, R.L. Jones, and B.C. Syrett, Chemical aspects of iodine-induced stress corrosion cracking of Zircaloys, [in] *Zirconium in the Nuclear Industry: Fifth International Symposium*, Boston, 1982.
[46] C. Gillen, A. Garner, A. Plowman, C.P. Race, T. Lowe, C. Jones, K.L. Moore, and P. Frankel, Advanced 3D characterisation of iodine induced stress corrosion cracks in zirconium alloys, *Mater. Charact.*, 141(2018), p. 348.
[47] B. Cox and R. Haddad, Recent studies of crack initiation during stress corrosion cracking of zirconium alloys, [in] *Zirconium in the Nuclear Industry: Seventh International Symposium*, Strasbourg, 1987.
[48] S.Y. Park, J.H. Kim, M.H. Lee, and Y.H. Jeong, Stress-corrosion crack initiation and propagation behavior of Zircaloy-4 cladding under an iodine environment, *J. Nucl. Mater.*, 372(2008), No. 2-3, p. 293.
[49] P. Jacques, F. Lefebvre, and C. Lemaignan, Deformation–corrosion interactions for Zr alloys during I-SCC crack initiation: Part I: Chemical contributions, *J. Nucl. Mater.*, 264(1999), No. 3, p. 239.
[50] T. Jezequel, Q. Auzoux, D.L. Boulch, M. Bono, E. Andrieu, C. Blanc, V. Chabretou, N. Mozzani, and M. Rautenberg, Stress corrosion crack initiation of Zircaloy-4 cladding tubes in an iodine vapor environment during creep, relaxation, and constant strain rate tests, *J. Nucl. Mater.*, 499(2018), p. 641.
[51] S.Y. Park, J.H. Kim, M.H. Lee, and Y.H. Jeong, Effects of the microstructure and alloying elements on the iodine-induced stress-corrosion cracking behavior of nuclear fuel claddings, *J. Nucl. Mater.*, 376(2008), No. 1, p. 98.
[52] S.Y. Park, J.H. Kim, B.K. Choi, and Y.H. Jeong, Crack initiation and propagation behavior of zirconium cladding under an environment of iodine-induced stress corrosion, *Met. Mater. Int.*, 13(2007), No. 2, p. 155.
[53] S.B. Farina, G.S. Duffó, and J.R. Galvele, Stress corrosion cracking of zirconium and Zircaloy-4 in iodine-alcoholic solutions, *Corrosion*, 59(2003), No. 5, p. 436.
[54] S.Y. Park, B.K. Choi, J.Y. Park, and Y.H. Jeong, Effect of hydride on the ISCC crack initiation and propagation in the high burnup-simulated nuclear fuel cladding, [in] *Proceedings of the Water Reactor Fuel Performance Meeting*, Paris, 2009.
[55] G.S. Duffó and S.B. Farina, Diffusional control in the intergranular corrosion of some hcp metals in iodine alcoholic solutions, *Corros. Sci.*, 47(2005), No. 6, p. 1459.
[56] R.B. Adamson, Effect of texture on stress corrosion cracking of irradiated zircaloy in iodine, *J. Nucl. Mater.*, 92(1980), No. 2-3, p. 363.
[57] W.S. Ryu, J.Y. Lee, Y.H. Kang, and H.C. Suk, Strain rate dependence of iodine-induced stress corrosion cracking of Zircaloy-4 under internal pressurization tests, *J. Mater. Sci.*, 25(1990), No. 7, p. 3167.
[58] M.R. Louthan, R.P. McNitt, and R.D. Sisson, Environmental degradation of engineering materials in hydrogen, [in] *Proceedings of Second International Conference on Environmental Degradation of Engineering Materials*, Blacksburg, 1981.
[59] M. Fregonese, C. Olagnon, N. Godin, A. Hamel, and T. Douillard, Strain-hardening influence on iodine induced stress corrosion cracking of Zircaloy-4, *J. Nucl. Mater.*, 373(2008), No. 1-3, p. 59.
[60] B. Meng, M.W. Fu, C.M. Fu, and K.S. Chen, Ductile fracture and deformation behavior in progressive microforming, *Mater. Des.*, 83(2015), p. 14.
[61] B. Cox and J.C. Wood, The mechanism of SCC of zirconium alloys in halogens, [in] *Proc. Int. Conf. on Mechanisms of Environment Sensitive Cracking of Materials*, Guildford, 1977, p. 520.
[62] L. Fournier, A. Serres, Q. Auzoux, D. Leboulch, and G.S. Was, Proton irradiation effect on microstructure, strain localization and iodine-induced stress corrosion cracking in Zircaloy-4, *J. Nucl. Mater.*, 384(2009), No. 1, p. 38.
[63] A. Serres, L. Fournier, M. Frégonèse, Q. Auzoux, and D. Leboulch, The effect of iodine content and specimen orientation on stress corrosion crack growth rate in Zircaloy-4, *Corros. Sci.*, 52(2010), No. 6, p. 2001.
[64] C. Gillen, A. Garner, C. Anghel, and P. Frankel, Investigating iodine-induced stress corrosion cracking of zirconium alloys using quantitative fractography, *J. Nucl. Mater.*, 539(2020), art. No. 152272.
[65] M.L. Rossi and C.D. Taylor, First-principles insights into the nature of zirconium-iodine interactions and the initiation of iodine-induced stress-corrosion cracking, *J. Nucl. Mater.*, 458(2015), p. 1.
[66] J.C. Wood, Factors affecting stress corrosion cracking of Zircaloy in iodine vapour, *J. Nucl. Mater.*, 45(1972), No. 2, p. 105.
[67] K. Une, Threshold values characterizing iodine-induced SCC of Zircaloys, *Res Mechanica*, 12(1984), No. 3, p. 161.
[68] S.B. Farina and G.S. Duffó, Intergranular to transgranular transition in the stress corrosion cracking of Zircaloy-4, *Corros. Sci.*, 46(2004), No. 9, p. 2255.
[69] C. Gillen, A. Garner, C. Jones, K.L. Moore, P. Tejland, and P. Frankel, High resolution crystallographic and chemical characterisation of iodine induced stress corrosion crack tips formed in irradiated and non-irradiated zirconium alloys, *J. Nucl. Mater.*, 519(2019), p. 166.
[70] E. Munch, L. Duisabeau, M. Fregonese, and L. Fournier, Acoustic emission detection of environmentally assisted cracking in Zircaloy-4 alloy, [in] *European Corrosion Conference: Long Term Prediction and Modelling of Corrosion*, Nice, 2004.
[71] C.M. Giordano, S.B. Farina, G.S. Duffó, and J.R. Galvele, Steric hindrance as a rate controlling step in stress corrosion cracking, *Corros. Sci.*, 49(2007), No. 6, p. 2745.
[72] C.R.F. Azevedo, Selection of fuel cladding material for nuclear fission reactors, *Eng. Fail. Anal.*, 18(2011), No. 8, p. 1943.
[73] J.C. Wood and J.R. Kelm, Effects of irradiation on the iodine-induced stress corrosion cracking of Candu Zircaloy fuel cladding, *Res. Mechanica*, 8(1983), No. 3, p. 127.
[74] C. Anghel, A.M.A. Holston, G. Lysell, S. Karlsson, R. Jakobsson, J. Flygare, S.T. Mahmood, D.L. Boulch, and A. Ioan, Experimental and finite element modeling parametric study for iodine-induced stress corrosion cracking of irradiated cladding, [in] *Proceedings of International Conference on Light Water Reactor Fuel Performance*, Orlando, Florida, 2010, p. 218.
[75] D.L. Boulch, L. Fournier, and C. Sainte-Catherine, Testing and modelling iodine-induced stress corrosion cracking in stress-relieved Zircaloy-4, [in] *Proceedings of the Seminar on*

Pellet–clad Interaction in Water Reactor Fuels, Aix-en-Provence, 2004.

[76] A.V.G. Sanchez, S.B. Farina, and G.S. Duffó, Effect of temperature on the stress corrosion cracking of Zircaloy-4 in iodine alcoholic solutions, *Corros. Sci.*, 49(2007), No. 7, p. 3112.

[77] D.B. Knorr, R.M. Pelloux, and L.F.P. Van Swam, Effects of material condition on the iodine SCC susceptibility of Zircaloy-2 cladding, *J. Nucl. Mater.*, 110(1982), No. 2-3, p. 230.

[78] M. Nagai, S. Shimada, S. Nishimura, K. Amano, and G. Yagawa, Elucidating the iodine stress corrosion cracking (SCC) process for zircaloy tubing, [in] *Proceedings of the Specialists' Meeting on Pellet Cladding Interaction in Water Reactor Fuel*, Seattle, 1983.

[79] K. Arioka, T. Yamada, T. Terachi, and G. Chiba, Influence of carbide precipitation and rolling direction on intergranular stress corrosion cracking of austenitic stainless steels in hydrogenated high-temperature water, *Corrosion*, 62(2006), No. 7, p. 568.

[80] P. Hofmann and J. Spino, Chemical aspects of iodine-induced stress corrosion cracking failure of Zircaloy-4 tubing above 50℃, *J. Nucl. Mater.*, 114(1983), No. 1, p. 50.

[81] R.L. Jones, D. Cubicciotti, and B.C. Syrett, Effects of test temperature, alloy composition, and heat treatment on iodine-induced stress corrosion cracking of unirradiated Zircaloy tubing, *J. Nucl. Mater.*, 91(1980), No. 2-3, p. 277.

[82] Y.S. Li, Y.H. Liu, G.B. Li, X.X. Dong, Y. Wang, Z.X. Gu, and Y.C. Zhang, Iodine-induced stress corrosion cracking behavior of alloy ZIRLO with Zr coatings by electrodepositing with different pulse current densities, *Corros. Sci.*, 193(2021), art. No. 109890.

[83] R.F. Mattas, F.L. Yaggee, and L.A. Neimark, Effect of zirconium oxide on the stress-corrosion susceptibility of irradiated Zircaloy cladding, [in] *Zirconium in the Nuclear Industry: Fifth International Symposium*, Boston, 1982.

[84] P.S. Sidky, Iodine stress corrosion cracking of Zircaloy reactor cladding: Iodine chemistry (a review), *J. Nucl. Mater.*, 256(1998), No. 1, p. 1.

[85] B. Gwinner, H. Badji-Bouyssou, M. Benoit, N. Brijiou-Mokrani, P. Fauvet, N. Gruet, P. Laghoutaris, F. Miserque, R. Robin, and M. Tabarant, Corrosion of zirconium in the context of the spent nuclear fuel reprocessing plant, [in] *21st International Conference and Exhibition Nuclear Fuel Cycle for a Low-carbon Future*, Paris, 2015.